Overlaying 10 Gb/s Legacy Optical Networks With 40 and 100 Gb/s Coherent Terminals

Oriol Bertran-Pardo, *Member, IEEE*, Jérémie Renaudier, *Member, IEEE*, Gabriel Charlet, *Member, IEEE*, Haïk Mardoyan, Patrice Tran, Massimiliano Salsi, *Member, IEEE*, and Sébastien Bigo, *Member, IEEE*

***Abstract*—We report on the upgrade at 40 Gb/s and 100 Gb/s of deployed legacy optical networks originally designed for 10-Gb/s nonreturn to zero (NRZ) on–off keying (OOK) data. These networks operate on a 50 GHz grid and incorporate periodically modules to compensate for chromatic dispersion. We discuss here the insertion of coherent polarization-division-multiplexed (PDM)-quadrature phase shift keying (QPSK) and PDM-binary PSK (BPSK) channels in legacy optical systems based on low chromatic dispersion fibers. We first assess the nonlinear tolerance of PDM-QPSK paired with coherent detection as a function of the bit rate. We also investigate the effect of optimizing the power of the PDM-QPSK channels independently of the power of copropagating OOK channels as well as introducing guard bands in the multiplex. We particularly show that 40 Gb/s PDM-QPSK data suffer larger performance penalties from copropagating 10 Gb/s OOK channels than 100 Gb/s data. Finally, we demonstrate that PDM-BPSK is a more attractive solution than PDM-QPSK at the bit rate of 40 Gb/s. Our experiments reveal that the BPSK-based solution is about 7.5 dB more robust to cross nonlinearities than the QPSK-based solution when inserted in one wavelength slot with 50 GHz spacing, originally designed for NRZ-OOK channels at 10 Gb/s.**

***Index Terms*—Binary phase shift keying (BPSK), coherent detection, digital signal processing, optical fiber communication, , quadrature phase shift keying (QPSK).**

I. Introduction

WIDELY deployed wavelength-division-multiplexed (WDM) optical networks operate at a channel bit rate of 10 Gb/s with nonreturn to zero (NRZ) on–off keying (OOK) modulation. These networks carry typically 10 Gb/s channels with a channel spacing of 50 GHz up to a maximum of 80 or 100 wavelength channels due to the limited bandwidth of current optical amplifiers. This represents a maximum capacity in the vicinity of 1 Tbit/s. Given that the traffic load currently approaches the maximum capacity of these networks, carriers plan to increase the total capacity of their network infrastructure by inserting spectrally efficient solutions at 40 or 100 Gb/s.

Moving from 10 to 40 Gb/s over an unchanged 50 GHz channel grid increases the information spectral density (i.e., the number of bits per second transmitted in a unit spectral band) from 0.2 to 0.8 bit/s/Hz. 40 Gb/s transponders are on the way to be cost-competitive with respect to 4×10 Gb/s and deployment has gained momentum for over three years in large carrier networks. Among all different solutions proposed to meet this challenge, coherent detection associated with DSP has attracted much attention [1], [2]. It enables polarization division multiplexing (PDM) to be fully exploited without the need of additional complexity at the receiver end [3]. Much interest has first been devoted to using PDM quadrature phase shift keying (QPSK) format paired with coherent detection at 40 Gb/s owing to the low required bandwidth and sampling rate of this solution. Unprecedented tolerance of 40 Gb/s coherent PDM-QPSK to linear impairments like polarization mode dispersion (PMD), chromatic dispersion (CD), and narrow filtering stemming from concatenation of reconfigurable optical add–drop multiplexers (ROADMs) has then been demonstrated experimentally [4]–[6]. This remarkable tolerance to linear impairments has paved the way for hero experiments at 100 Gb/s using coherent PDM-QPSK [7]–[9] demonstrating the potential to boost spectral efficiency up to 2 b/s/Hz. Further investigations have experimentally demonstrated spectrally efficient long-haul transmissions of 100 Gb/s coherent PDM-QPSK under the constraints of optically routed networks [10]–[14]. This solution is now considered as an attractive candidate to answer the predicted traffic growth of about 50% per year in optically routed transport systems [15].

However, most carriers do not intend to build a specific network for 40 or 100 Gb/s. One likely scenario for 10 Gb/s infrastructure upgrade is to design so-called hybrid systems. In these systems, several channels at 40 or 100 Gb/s are progressively inserted in wavelength slots with 50 GHz spacing (originally designed for NRZ channels at 10 Gb/s), transmitted over dispersion-managed links (i.e., incorporating periodically dispersion compensating modules to compensate for the accumulated dispersion along the line), and passed into 50 GHz based ROADMs. Different studies have addressed this key topic either by numerical simulations [16]–[18] and by laboratory experiments with offline processing [11], [19]–[23] and even with real-time processing on field trials [24], [25]. In this context, investigations have shown that transmission reach may be severely limited by cross nonlinear impairments stemming from the interactions with copropagating OOK channels [19], [20]. The majority of these studies relied on standard single-mode fiber (SSMF). However, the transmission reach reduction can be particularly emphasized over nonzero dispersion-shifted-fiber (NZDSF)-based systems owing to the low CD [23], [26]. Therefore, the potential of 40 and 100 Gb/s coherent solutions to

Manuscript received October 19, 2011; revised March 02, 2012; accepted April 26, 2012. Date of publication May 24, 2012; date of current version June 20, 2012.

The authors are with Alcatel-Lucent Bell Labs, 91620 Nozay, France (email: oriol.bertran_pardo@alcatel-lucent.com; jeremie.renaudier@alcatel-lucent.com; gabriel.charlet@alcatel-lucent.fr; haik.mardoyan@alcatel-lucent.com; patrice.tran@alcatel-lucent.com; massimiliano.salsi@alcatel-lucent.com; sebastien.bigo@alcatel-lucent.com).

Color versions of one or more of the figures in this paper are available online at http://ieeexplore.ieee.org.

Digital Object Identifier 10.1109/JLT.2012.2198432

overlay NZDSF-based legacy networks may significantly differ from that of SSMF-based systems.

In this paper, we report on a series of experiments conducted at 40 and 100 Gb/s using coherent PDM-binary phase shift keying (BPSK) and PDM-QPSK for overlaying legacy systems, expanding upon our initial results [20], [27], [28]. On top of that, it is difficult to draw a general picture with previous works in the literature since they address this topic with particular configurations that may differ from one another. We study here all the solutions over the same test bed for fair comparison and give an overview of the subject. We focus on an NZDSF system where degradations stemming from nonlinearities may be emphasized owing to the low CD.

This paper is organized as follows. Section II describes the experimental setup used along our investigations. In Section III, we investigate the tolerance to nonlinearities of a given modulation format at different bit rates, namely PDM-QPSK at 40 and 100 Gb/s. We discuss the impact of copropagating OOK channels onto the performance of coherent PDM-QPSK channels as a function of the relative channel power and frequency spacing. We show that PDM-QPSK can be considered as an attractive option at 100 Gb/s although it is not the most suitable choice for 40 Gb/s operation over legacy systems. Furthermore, we discuss the use of PDM-BPSK as an alternative solution for 40 Gb/s operation and demonstrate a 7.5 dB higher robustness against cross nonlinear impairments than PDM-QPSK in Section IV. Section V in turn discusses the results of this paper and gives an overview of the subject. Finally, Section VI concludes this paper. On top of that, the Appendix describes the signal processing used within the coherent receiver during our experiments.

II. Experimental Setup

A. Transmitter Setup

The experiments carried out here involve single-channel and WDM transmission. Two configurations are thus used at the transmitter side as shown in Fig. 1(a) and (b). In all configurations, the test channel (at 1546.52 nm) is PDM-QPSK modulated either at 100 or 40 Gb/s. On the contrary, the surrounding channels can be either kept continuous or NRZ modulated at 10 Gb/s corresponding to single-channel and WDM transmissions, respectively.

As depicted in Fig. 1, our transmitter consists of 82 distributed feedback (DFB) lasers, spaced by 50 GHz and separated into two spectrally interleaved combs which are independently modulated. To generate PDM-QPSK data, the light from each comb is sent to a different QPSK modulator operating at a symbol rate (R) of either 28 or 10.7 Gbaud. The modulators are fed by $2^{15}-1$ bit long pseudorandom bit sequences (PRBS) at 28 Gb/s (resp. 10.7 Gbaud), including forward error correction (FEC) and protocol overhead. QPSK data are then passed through a 50% return-to-zero (RZ) pulse carver operating at 28 GHz (resp. 10.7 GHz) in order to produce 28 Gbaud (resp. 10.7 Gbaud) RZ-QPSK signals. Polarization multiplexing is finally performed by dividing, decorrelating, and recombining the QPSK data through a polarization-maintaining 3 dB coupler, a polarization maintaining fiber (PMF), and a polarization beam combiner (PBC), respectively, with

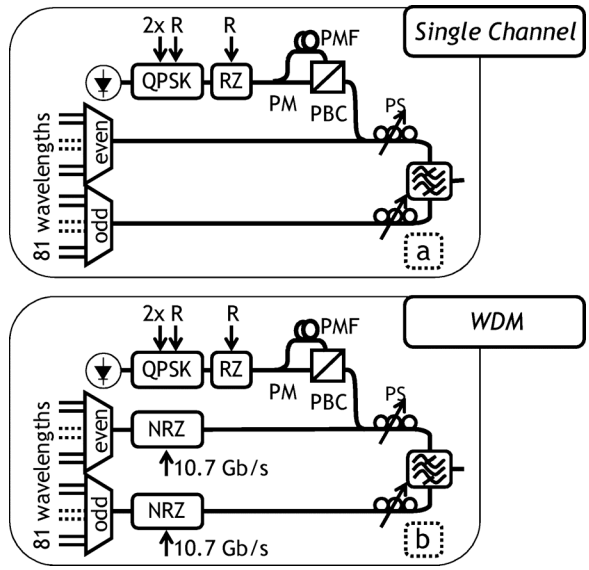

Fig. 1. Experimental transmitter setup for two different configurations: (a) single-channel and (b) WDM.

an approximate 10 ns delay, yielding PDM-QPSK data at 112 Gb/s (resp. 43 Gb/s).

To generate the 10 Gb/s NRZ data required for the hybrid WDM transmission experiment, the light from each comb is sent into a Mach–Zehnder modulator, fed by $2^{15}-1$ length PRBS at 10.7 Gb/s. In any case, the two generated combs are passed into a low-speed ($<$10 Hz) polarization scrambler (PS) and combined with a 50 GHz interleaver.

B. Link Configuration

The resulting multiplex is boosted through a dual-stage erbium-doped fiber amplifier (EDFA) incorporating dispersion compensating fiber (DCF) for precompensation and sent into the recirculating loop. The recirculating loop incorporates four 100 km long spans of NZDSF which are separated by dual-stage EDFA including an adapted spool of DCF for partial dispersion compensation, according to a typical terrestrial transmission map [29], as in [14], where the transmission fiber was SSMF. In contrast, here we used NZDSF with an effective area of 72 μm^2, a loss coefficient of 0.21 dB/km, and a CD of $\sim$4 ps/nm/km at 1550 nm. A wavelength selective switch is also inserted at the end of the loop to perform channel power equalization and can also emulate optical filtering and crosstalk stemming from nodes in transparent networks. This is done by passing odd and even channels through distinct output ports, introducing an additional optical path to even channels for further decorrelation (and thus a better emulation of an actual system) before recombining them through a 3 dB coupler.

We measure the performance after different transmission distances by changing the number of loop roundtrips and we vary the power per channel, Pch, at each fiber input by changing the output power of the amplifiers from 13 to 19 dBm, while keeping the number of channels constant at 82 channels. Since the maximum output power of the amplifiers is l9 dBm, we reduce the number of channels to extend the studied power range, when necessary. In all experiments, we chose to set the launch

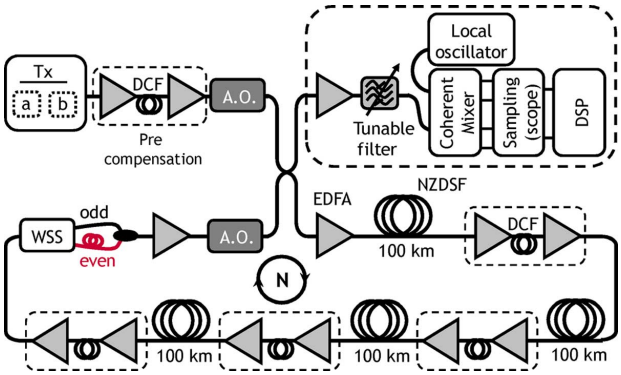

Fig. 2. Experimental recirculating loop setup and receiver setup (top-right inset).

power of the test channel at the same level as all the copropagating channels, unless explicitly mentioned.

C. Receiver Setup

At the receiver side, as seen in the top-right inset of Fig. 2, the channel under study is selected by a 0.4 nm bandwidth tunable filter and sent into the coherent receiver. Such a receiver consists of a polarization beam splitter followed by two coherent mixers, one for each received polarization state. Coherent mixers then combine the signal with a narrow linewidth ($\sim$100 kHz) tunable continuous wave laser achieving a phase offset of 90° between each one of their four outputs, so as to supply the in-phase and quadrature components of the signal. These waveforms are detected by four balanced photodiodes, digitized by four analog-to-digital converters (ADC) of an oscilloscope at 50 Gsamples/s with a 16 GHz electrical bandwidth, and stored by sets of 2 000 000 of samples (which corresponds to a time slot of 40 μs). Due to polarization scrambling, each recording corresponds to an arbitrary state of polarization at the input of the link.

Afterward, the waveforms are processed offline, as explained with more detail in the Appendix, for resampling at twice the symbol rate, digital CD mitigation, polarization demultiplexing by means of a constant modulus algorithm-based adaptive equalizer in a butterfly structure, and carrier phase recovery using the Viterbi and Viterbi algorithm.

III. Transmission Experiments Using PDM-QPSK

A. Impact of the Modulation Rate Onto the Tolerance to Interchannel Effects in Hybrid WDM Systems

The following experiments now focus on the tolerance of PDM-QPSK solutions at 40 and 100 Gb/s against interchannel nonlinear effects in hybrid WDM systems, in which 10 Gb/s NRZ channels coexist with PDM-QPSK ones. Thus, we measure the performance of one 100/40 Gb/s PDM-QPSK channel surrounded by 10 Gb/s NRZ channels [corresponding to the transmitter configuration depicted in Fig. 1(b)].

Fig. 3(a) shows the optical signal-to-noise ratio (OSNR) sensitivity for both 100 and 40 Gb/s PDM-QPSK. 40 Gb/s shows a 4 dB better noise sensitivity according to the ratio between the bit rates, 10log(40/100). Fig. 3(b) depicts the tolerance of 100 and 40 Gb/s PDM-QPSK to the impairments brought by 10 Gb/s NRZ copropagating channels after 800 km. The results obtained

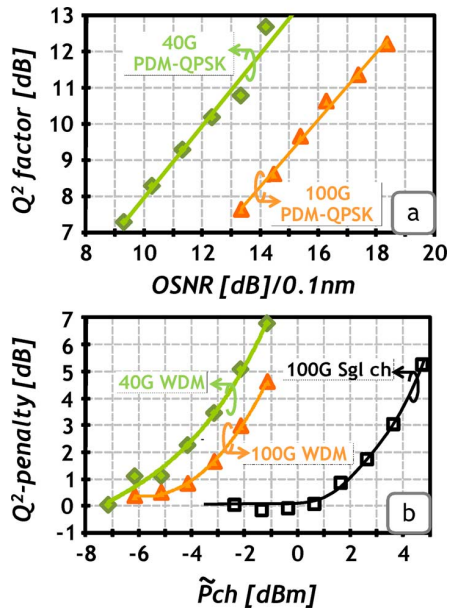

Fig. 3. (a) Optical noise sensitivity comparison between PDM-QPSK at 40 and 100 Gb/s and (b) tolerance to nonlinear effects in a hybrid (100 Gb/s-40 Gb/s mixed with 10 Gb/s NRZ) WDM transmission.

with 100 and 40 Gb/s PDM-QPSK do not exhibit the same tolerance against optical noise; in order to compare them thereby we represent in Fig. 3(b) the penalty in terms of Q^2 factor with respect to the performance obtained in back-to-back configuration at the same OSNR. As a reference, we also report in Fig. 3(b) the results obtained after 1200 km for a single-channel transmission at 100 Gb/s. To perform a fair comparison between the curves obtained at different distances, we define a relative normalized power as

$$\tilde{P}_{\mathrm{ch}} = P_{\mathrm{ch}} + 10\log(\mathrm{dist}/800)$$

where dist is the distance in kilometer.

For low values of $\tilde{P}_{\mathrm{ch}}$, performance is limited by optical noise and improves as far as OSNR is increased with the increase of $\tilde{P}_{\mathrm{ch}}$ and therefore no penalties are observed, as shown in Fig. 3(b) for single-channel transmission at 100 Gb/s. The intrachannel effects arise as soon as the launch power exceeds 1 dBm and 1 dB penalty is observed when $\tilde{P}_{\mathrm{ch}}$ reaches 2 dBm. As it can be observed in the WDM case, interchannel nonlinear effects brought by neighboring 10 Gb/s NRZ channels further reduce transmission performance of PDM-QPSK channels, indicating that performance of 100 Gb/s channels is here mainly limited by cross nonlinearities.

On top of that, the WDM performance at 40 Gb/s is further limited by cross nonlinearities stemming from neighboring 10 Gb/s NRZ channels as penalties arise for lower values of $\tilde{P}_{\mathrm{ch}}$, compared to 100 Gb/s. The better behavior against nonlinearities of PDM-QPSK at 100 Gb/s compared to that at 40 Gb/s is attributed to the equivalent filter of the digital phase estimation process in the coherent receiver that becomes more effective as the baud rate of the coherent-detected signal increases with respect to that of neighboring channels [30]. Indeed, when the baud rate of the coherent-detected channel is larger, the phase noise induced by cross nonlinear effects naturally presents a longer correlation over consecutive symbols, thus enabling a

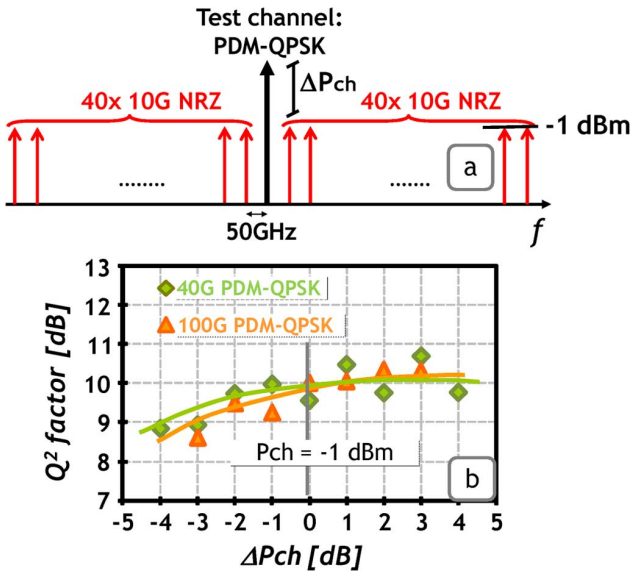

Fig. 4. (a) Channel configuration used and (b) performance of the test channel while varying its launch power around the power of 10 Gb/s NRZ channels fixed at −1 dBm after 800 km.

more accurate recovery of the carrier phase and a reduction of the interchannel-related impairments.

B. Containing Interchannel Effects in Hybrid WDM Systems

Next, we study the impact of optimizing the power of the PDM-QPSK channels independently of the power of copropagating OOK channels as well as introducing guard bands in the multiplex. We chose a power per channel of −1 dBm. This corresponds to typical values of 10G systems operating ultralong haul transport.

As shown in Fig. 3, performance of the PDM-QPSK channels is impacted noticeably when the power of all channels is set at −1 dBm. One possibility to improve the performance of a coherent PDM-QPSK channel in hybrid WDM configuration would be to optimize the power of the 40–100 Gb/s channel independently of the power of the 10G channels. Fig. 4(b) shows the performance evolution of the test channel while varying its launched power around the nominal value of −1 dBm after 800 km. We choose to represent in the *x*-axis the relative power of the test channel and we set as a reference the nominal power, i.e., −1 dBm.

It can be seen in Fig. 4 that below the nominal value, the increase of the launch power enables an increase of the performance. Once the nominal value is reached, only 0.25 dB increase in performance is obtained when increasing the launch power and consequently the OSNR by 3 dB beyond this nominal value of −1 dBm for 100 Gb/s and even less for 40 Gb/s channel. This performance limitation suggests that the coherent PDM-QPSK channel suffers severe nonlinear penalties arising from the copropagating 10 Gb/s NRZ channels [31] that are not recovered by increasing the received OSNR. Therefore, the degree of freedom consisting in optimizing the channel power of the inserted channel almost vanishes in this configuration.

Another option to contain the penalties brought by copropagating channels on the performance of coherent PDM-QPSK channels in hybrid WDM configuration is to introduce guard bands between coherent PDM-QPSK and 10 Gb/s NRZ channels. This option was already investigated in [20] to overcome penalties brought by 10 Gb/s NRZ channels onto a coherent PDM-QSPK channel operating at 40 Gb/s over an SSMF-based system. However, a limited guard band as large as 300 GHz was not sufficient to recover the penalties due to interchannel effects induced by 10 Gb/s NRZ channels in that experiment. Since interchannel effects appear to be less penalizing when increasing bit rate from 40 to 100 Gb/s, we aim here at measuring and comparing the required guard band for the insertion of a coherent PDM-QPSK channel at both 40 and 100 Gb/s with only 1 dB performance penalty.

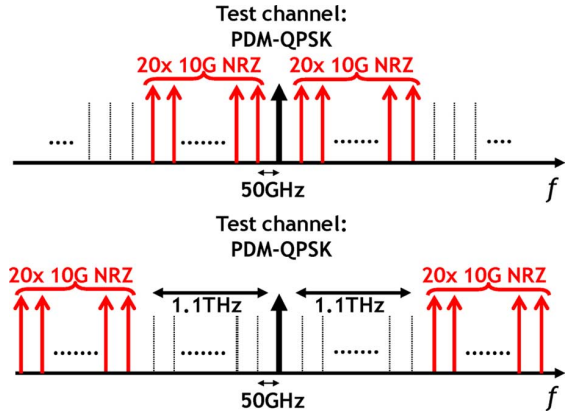

Fig. 5. Channel allocation used when moving away neighbor channels.

As depicted in Fig. 5, we investigate this option by gradually moving away two sets of 20 adjacent channels on both sides of the 100 Gb/s test channel up to 1.1 THz. Ideally, when surrounding channels are far enough from the test one, the performance of the test channel should be the same as in a single-channel transmission. The total number of channel is kept constant and the output power of inline amplifiers is set at 15 dBm, corresponding to a launch power of −1 dBm per channel.

We contain here the power of the 40 Gb/s test channel at −5 dBm (4 dB lower than that of the 100 Gb/s channel), in order to obtain approximately the same performance in single-channel transmission and to ease comparisons. In the meantime, the power of the 10 Gb/s NRZ channels is kept at −1 dBm to ensure that the test channel at 40 Gb/s experiments the same amount of interchannel effects as at 100 Gb/s.

The results of these measurements after 800 km for both 40 and 100 Gb/s coherent PDM-QPSK channels are depicted in Fig. 6. Two different behaviors can be observed. First, performance increases rapidly when increasing the guard band for relatively small values of guard band. This indicates that performance is mainly limited by cross-phase modulation (XPM) when 10 Gb/s channels are close to the PDM-QPSK channels [32], [33].

Second, we observe a slow increase of performance up to a channel spacing of 1 THz. We attribute this weak dependence of the performance on the guard band mainly to nonlinear cross-polarization scattering (sometimes also referred as cross-polarization modulation [34], [35]) induced by surrounding 10 Gb/s NRZ channels. In fact, copropagating channels distant by more than 500 GHz cause nonnegligible nonlinear degradations on

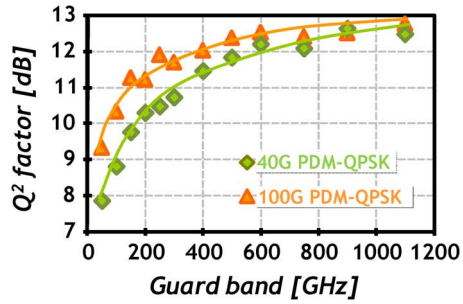

Fig. 6. Performance evolution versus guard band around PDM-QPSK channel after 800 km transmission for 100 Gb/s (orange triangles) in a hybrid WDM configuration and 40 Gb/s (green diamonds).

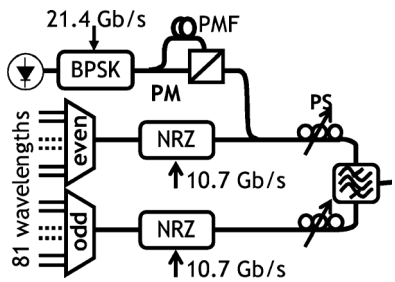

Fig. 7. Experimental setup for long-haul transmission system based on NZDSF transmission link.

coherent PDM-QPSK signals, contrary to conventional 10 Gb/s receivers using polarization-insensitive detection [33].

Nonlinear cross-polarization scattering creates sudden changes of the states of polarization (SOP) of the signal and is weakly dependent on the channel spacing [20], [36]. Such changes of the SOP are possibly faster than the speed of the (digital) polarization tracking done in polarization-sensitive receivers [35]. Thus, in a polarization-sensitive receiver, these changes in SOP may be translated into amplitude fluctuations deteriorating the performance, whereas they would not affect the performance of a polarization insensitive receiver.

However, it can be seen that 100 Gb/s PDM-QPSK is clearly less impacted by impairments brought by 10 G/s NRZ neighbors than 40 Gb/s PDM-QPSK. The largest penalties are induced by the closest adjacent channels, due to the effect of CPM. The maximum impact of nonlinearities is observed, as expected, when no guard band separate the 10G NRZ channels from the test channel, corresponding to a minimum 50 GHz spacing. This penalty is about 4 dB at 100 Gb/s, whereas it exceeds 5 dB at 40 Gb/s, thus highlighting the lower tolerance of the 40 Gb/s solution against interchannel effects [30], [31]. Moreover, the guard band required to ensure less than 2 dB penalty in the performance of the 100 Gb/s channel is of 150 GHz, whereas at 40 Gb/s, twice larger guard band is required, i.e., 300 GHz.

Compared to the possibility of optimizing the power of the PDM-QPSK channels independently of the power of copropagating OOK channels studied in Fig. 4, introducing guard bands in the multiplex appears to be more effective, mainly at 100 Gb/s. Indeed, the total transmitted capacity of the system should be drastically reduced to ensure correct performance of 40 Gb/s PDM-QPSK in a hybrid 10G/40G WDM system, whereas at 100 Gb/s a narrower bandgap could be considered.

IV. Long-Haul Transmission of 40 Gb/s Channel Over Legacy System Using PDM-BPSK

A. Robustness Against Interchannel Effects in Hybrid WDM Systems

Cross nonlinear interactions stemming from copropagating 10 Gb/s channels are a major issue when upgrading legacy systems with 40 Gb/s PDM-QPSK channels according to previous results. In this context, the use of PDM binary phase shift keying (BPSK) coherent solution has been recently reported. Originally proposed for undersea transmissions [37], PDM-BPSK has been shown as an attractive candidate for long-haul applications over legacy systems [38], [39], at the expense of doubling bandwidth requirements and sampling rate of the coherent receiver.

We performed another set of transmission experiments to fairly compare the nonlinear tolerance of these two solutions under the same conditions, i.e., over a system relying on low dispersion fiber carrying 10 Gb/s NRZ channels. We modulate the studied channel through a BPSK modulator fed with a $2^{15}-1$ bit long PRBS. The modulator operates at 21.4 Gb/s including FEC overhead. Polarization multiplexing is emulated by splitting the signal along two paths, delaying one of the two with a section of PMF, and recombining the two paths using a polarization beam combiner leading to 40 Gb/s PDM-BPSK data. The test channel is then coupled into the even comb.

Besides, 81 DFB lasers spaced by 50 GHz are again separated in even and odd combs and independently modulated with 10.7 Gb/s NRZ, as explained in Section II. The resulting submultiplex is passed into a PS and then it is spectrally interleaved with the odd comb (also polarization scrambled). The resulting multiplex is boosted through a dual-stage EDFA incorporating DCF for precompensation and sent into the recirculating loop described in Fig. 2. At the receiver side, the channel under study is selected by a 0.4 nm bandwidth tunable filter and sent into the coherent receiver. Compared to the digital processing chain described in the Appendix for PDM-QPSK, only a slight modification has to be done for constant modulus algorithm (CMA)-based polarization demultiplexing according to [40].

Fig. 8 represents the tolerance of 40 Gb/s PDM-BPSK to impairments brought by 10 Gb/s NRZ copropagating channels after 2800 km in terms of Q^2 factor penalty with respect to the performance obtained in back-to-back configuration at the same OSNR versus the normalized power as defined in Section III-A. As a reference, we also report the results obtained after 2400 km of single-channel transmission at 40 Gb/s PDM-BPSK. The single-channel results were obtained by removing the modulation of the surrounding channels.

As previously stated, performance is limited by optical noise for low values of power per channel and therefore no penalties are observed when power increases up to a certain value. Comparing the results obtained in single-channel configuration and in WDM configuration, we observe that performance is also, here, mainly limited by cross nonlinearities for high power values. Nevertheless, PDM-BPSK appears to be more robust against penalties induced by copropagating channels than PDM-QPSK.

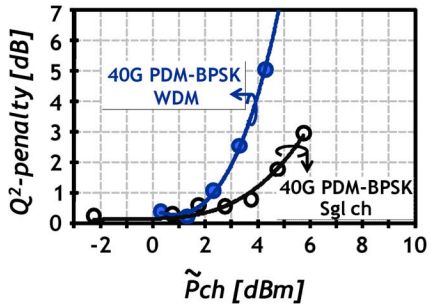

Fig. 8. Performance of coherent PDM-BPSK in a hybrid WDM configuration over NZDSF.

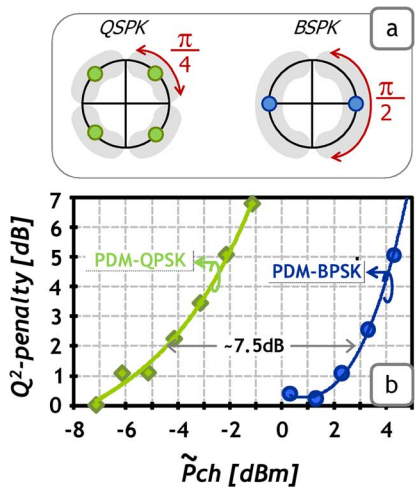

Fig. 9. (a) Schematic representation of constellation diagram and tolerable phase error for BPSK and QPSK signals. (b) Nonlinear tolerance comparison between coherent PDM-BPSK and PDM-QPSK solutions in a hybrid 10G/40G WDM configuration.

B. Comparison With 40 Gb/s PDM-QPSK

To compare fairly the tolerance of PDM-QPSK and PDM-BPSK at 40 Gb/s to nonlinearities stemming from copropagating 10 Gb/s channels, Fig. 9(b) depicts the Q^2 factor penalty versus the normalized power, as defined previously. This figure clearly shows that PDM-BPSK is more robust than PDM-QPSK against interchannel nonlinearities brought by neighboring NRZ channels since they become penalizing for much higher powers. The power corresponding to a 2 dB penalty is around -4.5 dBm for PDM-QPSK, whereas for PDM-BPSK this power is about 7.5 dB higher. This large tolerance discrepancy against nonlinear effects is even greater than that observed over SSMF in [38] because of the low local CD of our transmission fiber. This highlights the potential of the coherent PDM-BPSK at 40 Gb/s solution for long-haul applications over dispersion-managed systems based on low dispersion fiber. This better tolerance of PDM-BPSK against nonlinearities is mainly attributed to the fact that, compared to PDM-QPSK, it has twice as large phase shift between symbols, which allows to tolerate twice as large phase errors [see Fig. 9(a)], and also to the fact that it has twice as large symbol rate [17].

V. Discussion

PDM-BPSK and PDM-QPSK benefit from the high sensitivity associated with (homodyne) coherent detection and the possibility of compensating for linear impairments thanks to dedicated DSP. Moreover, both of them allow increasing the information spectral density of today's 10 Gb/s networks from 0.2 to 0.8 b/s/Hz. PDM QPSK has two clear advantages compared to PDM BPSK: the lower symbol rate and the narrower spectrum. The narrower spectrum makes PDM-QPSK inherently more tolerant to narrow optical filtering, which can be used to tightly pack 40 Gb/s PDM-QPSK in ultradense WDM configurations with a channel spacing smaller than 50 GHz. Such ultradense WDM configurations allows further increasing the spectral efficiency beyond 0.8 b/s/Hz but are, in general, more sensitive to interchannel nonlinearities due to the small channel spacing. The lower symbol rate of PDM-QPSK in turn relaxes the constraints on the bandwidth and speed requirements of high-speed electronic devices and ADCs. This could result in an easier and more cost-effective practical implementation. However, PDM-QPSK at 40 Gb/s is highly vulnerable against nonlinear-induced phase distortions stemming from 10 Gb/s copropagating channels.

PDM-BPSK is more tolerant against nonlinearities coming from copropagating channels, by up to 7.5 dB. The use of PDM-BPSK increases significantly the system reach with respect to PDM-QPSK which is clearly its most undeniable comparative advantage. Moreover, PDM-BPSK, operating at 21.4 Gbaud, benefits from the large-scale development of the 100 Gb/s PDM-QPSK, which operates at 28 Gbaud. This allows overcoming practical implementation issues and therefore PDM-BPSK is likely to be the most suitable solution for terrestrial systems covering long distances at 40 Gb/s.

Reaching the upgrade of legacy networks at 100 Gb/s with PDM-BPSK at 100 Gb/s is nowadays very challenging because of its broad spectrum ($\sim$100 GHz) which does not easily fit into the standard 50 GHz grid. Moreover, PDM-BPSK presents stringent requirements on bandwidth and speed of electronic devices and ADCs, due the high symbol rate of 56 Gbaud which would be required.

PDM-QPSK appears as a better candidate for upgrading 50 GHz grid legacy systems. It has a symbol rate of 28 Gbaud (relaxing thus the requirements on opto-electronics) and a main-lobe spectrum width of 56 GHz compatible with the 50 GHz channel spacing. The combination of 100 Gb/s PDM-QPSK with a 50 GHz grid enables a tenfold increase, with respect to 10 Gb/s systems, in information spectral density reaching long-haul transmissions with 2 b/s/Hz.

VI. Conclusion

We have investigated in this paper the tolerance to intrachannel and interchannel nonlinearities of coherent systems at 40 and 100 Gb/s. We have paid particular attention to the upgrade of optical networks designed for 10 Gb/s operations. In that respect, we have characterized the robustness of PDM-BPSK at 40 Gb/s and PDM-QPSK at 40 and 100 Gb/s to nonlinear effects stemming from 10 Gb/s NRZ copropagating channels. We have shown that coherent PDM-QPSK channels at 40 Gb/s are significantly more impacted than at 100 Gb/s. We have considered two possible options to contain the impact of nonlinearities caused by 10 Gb/s NRZ copropagating channels. Optimizing the power of the coherent channels independently of the power of copropagating channels brings almost no benefits since the increase of the OSNR of coherent channels is not

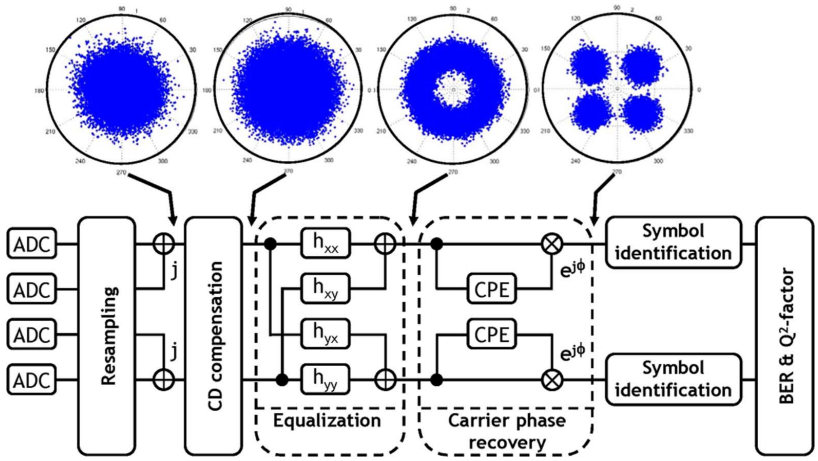

Fig. 10. DSP done in coherent receiver.

translated in better performance when operating under typical conditions designed for 10 Gb/s operation. On the contrary, the introduction of guard bands in the multiplex can partially contain nonlinear penalties caused by neighboring 10 Gb/s NRZ channels and it is more efficient at 100 Gb/s than at 40 Gb/s. More precisely, we have demonstrated that leaving a 150 GHz guard band would provide a beneficial 2 dB improvement of Q^2 factor margins at 100 Gb/s. Finally, we have shown that PDM-BPSK is more robust that PDM-QPSK at 40 Gb/s while being compatible with 50 GHz grid. This highlights the potential of the coherent PDM-BPSK at 40 Gb/s solution for long-haul applications over dispersion-managed systems based on low dispersion fiber.

APPENDIX
DIGITAL SIGNAL PROCESSING FOR COHERENT RECEIVERS

By providing access to the amplitude, the phase, and the polarization of the optical field, coherent receivers enjoy the high sensitivity associated with homodyne detection with the added benefits of DSP. In the following, we briefly describe the major steps of such a DSP.

1) Retiming: According to the Shannon–Nyquist criterion, the received signal should be sampled at a rate of at least twice its bandwidth. Practically, in a transponder specially designed for coherent systems, the 3 dB bandwidth of the ADC is roughly 0.5–0.8 times the symbol rate and the ADC sampling rate is exactly twice the symbol rate. Nevertheless, sampling heads used in most of the research experiments have a 3 dB bandwidth of 16 GHz and work at a fixed sampling rate slightly lower than twice the symbol rate. Here, this sampling rate is 50 Gsamples/s for a symbol rate of 28 Gbaud as noted in [8] and [9]. Consequently, digitized signals have roughly 1.8 samples per symbol. In order to have DSP operating at exactly two samples per symbol, we oversample the signal using an interpolation technique and extract the tone at the symbol rate $(1/\mathrm{T})$ from the spectrum of the magnitude-squared signal. We subsequently upsample the signal from 1.8 to 2 synchronously using the recovered clock.

2) CD Compensation: CD is a static polarization-independent phenomenon and, then, it can be compensated for before equalizing and demultiplexing the received signal to recover the two orthogonal polarization tributaries sent at the transmitter side. Thus, since we roughly know the residual amount of CD, we can use the well-known analytical expression of CD to design the filter which compensates for it. This expression is

$$G(z,\omega) = \exp\left(-j\frac{Dz\lambda^2}{4\pi c}\omega^2\right)$$

where z is the distance, ω is the angular frequency, j is the imaginary unit, D is the dispersion coefficient of the fiber, λ is the wavelength, and c is the speed of light. The practical implementation of the digital filter corresponding to such an expression is impossible because its response is not causal and has an infinite duration. Practically, the response is truncated and static finite impulse response (FIR) filters are used. The length of these filters is proportional to the amount of CD to be compensated for.

3) Equalization and Polarization Demultiplexing: A key part of the DSP is to demultiplex the received signal to recover the two orthogonal polarization tributaries sent at the transmitter side. This can be done using blind adaptive FIR filters updated using stochastic gradient CMA as proposed in [41]. The filters are arranged in a butterfly structure (as seen in Fig. 10) and are continuously updated to follow channel perturbations like polarization-dependent fluctuations, PMD, etc. The impact of all these perturbations can be modeled as a Jones matrix. It has to be noted that the two input signals of the block x_{in} and y_{in} are a mix of the two signals emitted along the two orthogonal SOP of the light. Therefore, the task of the equalizer is to estimate the inverse of the Jones matrix so as to reverse the effects induced by the channel propagation. The output signal is obtained as follows:

$$x_{\mathrm{out}} = h_{xx}\cdot x_{\mathrm{in}} + h_{xy}\cdot y_{\mathrm{in}}$$
$$y_{\mathrm{out}} = h_{yx}\cdot x_{\mathrm{in}} + h_{yy}\cdot y_{\mathrm{in}}$$

where x_{in} and y_{in} are the input signals, x_{out} and y_{out} are the output signals, and h_{xx}, h_{xy}, h_{yx}, and h_{yy} are the adaptive FIR filters having $\mathrm{T}/2$-spaced complex tap coefficients (also simply known as taps). These coefficients are updated such that

$$h_{xx} \rightarrow h_{xx} + \mu\varepsilon_x x_{\mathrm{out}}\cdot x_{\mathrm{in}}^*$$
$$h_{xy} \rightarrow h_{xy} + \mu\varepsilon_y y_{\mathrm{out}}\cdot y_{\mathrm{in}}^*$$
$$h_{yx} \rightarrow h_{yx} + \mu\varepsilon_x x_{\mathrm{out}}\cdot x_{\mathrm{in}}^*$$

$$h_{yy} \rightarrow h_{yy} + \mu\varepsilon_y y_{\text{out}} \cdot y_{\text{in}}^*$$

where μ is the convergence parameter, x_{in}^* and y_{in}^* are the complex conjugate of x_{in} and y_{in}, respectively, and the error terms which have to be minimized are given by

$$\varepsilon_x = 1 - |x_{\text{out}}|^2$$
$$\varepsilon_y = 1 - |y_{\text{out}}|^2$$

for unit amplitude signals. At the end of this DSP block, the two output signals x_{out} and y_{out} are polarization-demultiplexed and equalized thanks to the estimation of the Jones matrix.

It must be noted here that, using complex tap-coefficients, a 13-taps adaptive equalizer also mitigates for any residual CD of up to ± 750 ps/nm at 100 Gb/s [9].

Once the two polarization tributaries have been separated by the blind adaptive equalizer, phase tracking has to be done in the digital domain since the local oscillator is not optically phase locked onto the received signal. Otherwise, the constellation diagram expected (four clouds located at $+\pi/4,\ +3\pi/4,\ -3\pi/4$, and $-\pi/4$) would look like a thick circle, as it appears at the output of the polarization demultiplexing stage in Fig. 10. This phase offset will be recovered by the following block in the DSP. Compared to the digital processing chain described for PDM-QPSK, a slight modification has to be done for polarization demultiplexing as described in [40].

4) Carrier Phase Estimation (CPE): The CPE is used to recover and subsequently remove the remaining phase mismatch ϕ between the local oscillator and the signal. Since the previous adaptive algorithm acts as a fine clock recovery block as well, the estimation of this mismatch is done on the "central" sample only (while the other is dropped) by using a nonlinear carrier phase tracking algorithm [42] as follows: first, the Mth power of the complex symbol is taken in order to remove any information encoded in the phase of the signal (M being the number of phase levels of the modulation, i.e., four for a QPSK modulation). Second, an averaging window of $N+1$ elements is computed by summing the result over $N/2$ precursor and $N/2$ postcursor symbols. Then, the argument is taken since we are only interested in the phase. Finally, as shown by the following equation, the resulting phase is divided by M to correct for the initial elevation to the Mth power and subsequently unwrapped to obtain results in the range $]-\pi, \pi]$

$$\hat{\phi}(k) = \frac{1}{M} \arg \left[\sum_{p=-N/2}^{N/2} x_{\text{out}}^M (k+p) \right].$$

This step has been shown to be critical since a correct estimation of the phase depends on the number of consecutives symbols considered [19], [20]. In fact, when transmission performance is limited mainly by Gaussian noise, high values of N can be employed to obtain better performance. In contrast, when nonlinear effects become dominant during the transmission, a smaller number of consecutive symbols should be considered to follow fast variations of the phase, thus reducing the accuracy of the phase estimation.

It has to be noted here that, as pointed out in [43], phase estimators perform well when estimated phase can be considered as unbiased in the range of the chosen averaging window, leading to the following condition on the frequency detuning Δf between the carrier of the received signal and the frequency of the local oscillator:

$$\Delta f \leq \frac{1}{2(N+1)MT_s}$$

where T_S is the sampling period, $N+1$ is the averaging window of CPE, and M is the number of symbol states. Note here that a typical averaging window of 11 elements yields a maximum tolerable frequency offset around ± 300 MHz for 100 Gb/s PDM-QPSK operating at 28 Gbaud. Since the accuracy of typical temperature-stabilized lasers is around $+/-1.5$ GHz, a technique derived from the nonlinear carrier phase tracking algorithm and presented in [43] is usually performed to estimate and remove the frequency detuning Δf before processing CPE.

5) Symbol Identification and Bit-Error-Ratio Calculation: After CPE, the digital signal is ready to be processed by the decision block. Finally, we compare the extracted pattern with the original sequence, errors are found and counted. This results in a bit error rate (BER). For practical reasons, the system performance measured is usually not expressed in BER but in Q^2 factor. Here, the resulting BER of at least four recordings is averaged before being transformed into Q^2 factors.

REFERENCES

[1] M. G. Taylor, "Coherent detection method using DSP for demodulation of signal and subsequent equalization of propagation impairments," *IEEE Photon. Technol. Lett.*, vol. 16, no. 2, pp. 674–676, Feb. 2004.

[2] D.-S. Ly-Gagnon, S. Tsukamoto, K. Katoh, and K. Kikuchi, "Coherent detection of optical quadrature phase shift keying signals with carrier phase estimation," *J. Lightw. Technol.*, vol. 24, no. 1, pp. 12–21, Jan. 2006.

[3] S. J. Savory, A. D. Stewart, S. Wood, G. Gavioli, M. G. Taylor, R. I. Killey, and P. Bayvel, "Digital equalisation of 40 Gb/s per wavelength transmission over 2480 km of standard fibre without optical dispersion compensation," presented at the Eur. Conf. Opt. Commun., Cannes, France, Jan. 2006, Paper Th2.5.5.

[4] S. J. Savory, "Digital filters for coherent optical receivers," *Opt. Exp.*, vol. 16, no. 2, pp. 804–817, Jan. 2008.

[5] J. Renaudier, G. Charlet, M. Salsi, O. Bertran-Pardo, H. Mardoyan, P. Tran, and S. Bigo, "Linear fiber impairments mitigation of 40 Gbit/s polarization-multiplexed QPSK by digital processing in a coherent receiver," *J. Lightw. Technol.*, vol. 26, no. 1, pp. 36–42, Jan. 2008.

[6] C. Laperle, B. Villeneuve, Z. Zhang, D. McGhan, H. Sun, and M. O'Sullivan, "Wavelength division multiplexing and polarization mode dispersion performance of a coherent 40 Gb/s dual-polarization quadrature phase shift keying transceiver," presented at the Opt. Fiber Commun. Conf., Anaheim, CA, Paper PDP16.

[7] G. Charlet, M. Salsi, P. Tran, M. Bertolini, H. Mardoyan, J. Renaudier, O. Bertran-Pardo, and S. Bigo, "72 × 100 Gb/s transmission over transoceanic distance, using large effective area fiber, hybrid Raman-erbium amplification and coherent detection," presented at the Opt. Fiber Commun. Conf., San Diego, CA, Paper PDPB6.

[8] G. Charlet, J. Renaudier, H. Mardoyan, P. Tran, O. Bertran-Pardo, F. Verluise, M. Achouche, A. Boutin, F. Blache, J.-Y. Dupuy, and S. Bigo, "Transmission of 16.4 Tbit/s capacity over 2 550 km using PDM QPSK modulation format and coherent receiver," presented at the Opt. Fiber Commun. Conf., San Diego, CA, Paper PDP3.

[9] C. R. S. Fludger, T. Duthel, D. van den Borne, C. Schulien, E.-D. Schmidt, T. Wuth, J. Geyer, E. De Man, G.-D. Khoe, and H. de Waardt, "Coherent equalization and POLMUX-RZ-DQPSK for robust 100-GE transmission," *J. Lightw. Technol.*, vol. 26, no. 1, pp. 64–72, Jan. 2008.

[10] J. Renaudier, G. Charlet, O. Bertran-Pardo, H. Mardoyan, P. Tran, M. Salsi, and S. Bigo, "Experimental analysis of 100 Gb/s coherent PDM-QPSK long-haul transmission under constraints of typical terrestrial networks," presented at the Eur. Conf. Opt. Commun., Brussels, Belgium, Paper Th 2.A.3.

[11] M. S. Alfiad, D. van den Borne, T. Wuth, M. Kuschnerov, B. Lankl, C. Weiske, E. de Man, A. Napoli, and H. de Waardt, "111-Gb/s POLMUX-RZ-DQPSK transmission over 1140 km of SSMF with 10.7-Gb/s NRZ-OOK neighbours," presented at the Eur. Conf. Opt. Commun., Brussels, Belgium, Paper Mo.4.E.2.

[12] J. Renaudier, O. Bertran-Pardo, H. Mardoyan, P. Tran, M. Salsi, G. Charlet, and S. Bigo, "Impact of temporal interleaving of polarization tributaries onto 100 Gb/s coherent transmission systems with RZ pulse carving," *IEEE Photon. Technol. Lett.*, vol. 20, no. 24, pp. 2036–2038, Dec. 2008.

[13] M. S. Alfiad, D. van den Borne, S. L. Jansen, T. Wuth, M. Kuschnerov, G. Grosso, A. Napoli, and H. de Waardt, "111-Gb/s POLMUX-RZ-DQPSK transmission over LEAF: Optical versus electrical dispersion compensation," presented at the Opt. Fiber Commun. Conf., San Diego, CA, Paper OThR4.

[14] O. Bertran-Pardo, J. Renaudier, G. Charlet, P. Tran, H. Mardoyan, M. Salsi, and S. Bigo, "Experimental assessment of interactions between nonlinear impairments and polarization-mode dispersion in 100-Gb/s coherent systems versus receiver complexity," *IEEE Photon. Technol. Lett.*, vol. 21, no. 1, pp. 51–53, Jan. 2009.

[15] "An Overview: The Next Generation of Ethernet," IEEE 802.3 Higher Speed Study Group Tutorial, IEEE 802 Plenary. Atlanta, GA, Nov. 12, 2007 [Online]. Available: http://www.ieee802.org/3/hssg/public/nov07/HSSG_Tutorial_1107.zip, Inst. Electr. Electron. Eng

[16] C. Xie, "Impact of nonlinear and polarization effects on coherent systems," *Opt. Exp.*, vol. 19, no. 26, pp. B915–B930, Dec. 2011.

[17] A. Bononi, N. Rossi, and P. Serena, "Transmission limitations due to fiber nonlinearity," presented at the Opt. Fiber Commun. Conf., Los Angeles, CA, Paper OWO7.

[18] D. Rafique, M. Forzati, and J. Mårtensson, "Impact of nonlinear fibre impairments in 112 Gb/s PM-QPSK transmission with 43 Gb/s and 10.7 Gb/s neighbours," in *Proc. 12th Int. Conf. Transparent Opt. Netw.*, Munich, Germany, 2010, pp. 1–4, Paper We.D16.

[19] D. van den Borne, C. R. S. Fludger, T. Duthel, T. Wuth, E. D. Schimidt, C. Schulien, E. Gottwald, G. D. Khoe, and H. de Waardt, "Carrier phase estimation for coherent equalization of 43-Gb/s POLMUX-NRZ-DQPSK transmission with 10.7-Gb/s NRZ neighbours," presented at the Eur. Conf. Opt. Commun., Berlin, Germany, 2007, Paper We7.2.3.

[20] O. Bertran-Pardo, J. Renaudier, G. Charlet, H. Mardoyan, P. Tran, and S. Bigo, "Nonlinearity limitations when mixing 40 Gb/s coherent PDM-QPSK channels with preexisting 10 Gb/s NRZ channels," *IEEE Photon. Technol. Lett.*, vol. 20, no. 15, pp. 1314–1316, Aug. 1, 2008.

[21] J. Renaudier, G. Charlet, O. Bertran-Pardo, H. Mardoyan, P. Tran, M. Salsi, and S. Bigo, "Transmission of 100 Gb/s coherent PDM-QPSK over 16×100 km of standard fiber with all-erbium amplifiers," *Opt. Exp.*, vol. 17, no. 7, pp. 5112–5119, Mar. 2009.

[22] M. S. Alfiad, D. van den Borne, T. Wuth, M. Kuschnerov, B. Lankl, C. Weiske, E. de Man, A. Napoli, and H. de Waardt, "111-Gb/s POLMUX-RZ-DQPSK transmission over 1140 km of SSMF with 10.7-Gb/s NRZ-OOK neighbours," presented at the Eur. Conf. Opt. Commun., Brussels, Belgium, 2008, Paper Mo.4.E.2.

[23] M. S. Alfiad, D. van den Borne, S. L. Jansen, T. Wuth, M. Kuschnerov, G. Grosso, A. Napoli, and H. de Waardt, "111-Gb/s POLMUX-RZ-DQPSK transmission over LEAF: Optical versus electrical dispersion compensation," presented at the Opt. Fiber. Commun. Conf., San Diego, CA, 2009, Paper OThR4.

[24] M. Birk, P. Gerard, R. Curto, L. Nelson, X. Zhou, and P. Magill, "Field trial of a real-time, single wavelength, coherent 100 Gbit/s PM-QPSK channel upgrade of an installed 1800 km link," presented at the Opt. Fiber Commun. Conf., San Diego, CA, 2010, Paper PDPD1.

[25] M. Birk, P. Gerard, R. Curto, L. E. Nelson, X. Zhou, P. Magill, T. J. Schmidt, C. Malouin, B. Zhang, E. Ibragimov, S. Khatana, M. Glavanovic, R. Lofland, R. Marcoccia, R. Saunders, G. Nicholl, M. Nowell, and F. Forghieri, "Real-Time single-carrier coherent 100 Gb/s PM-QPSK field trial," *J. Lightw. Technol.*, vol. 29, no. 4, pp. 417–425, Feb. 2011.

[26] C. Xia, J. F. Pina, A. Striegler, and D. van den Borne, "On the nonlinear threshold of polarization-multiplexed QPSK transmission with different dispersion maps," presented at the Eur. Conf. Opt. Commun., Geneva, Switzerland, 2011, Paper We.10.P1.63.

[27] J. Renaudier, O. Bertran-Pardo, H. Mardoyan, P. Tran, M. Salsi, G. Charlet, and S. Bigo, "Investigation on WDM nonlinear impairments arising from the insertion of 100-Gb/s coherent PDM-QPSK over legacy optical networks," *IEEE Photon. Technol. Lett.*, vol. 21, no. 24, pp. 1816–1818, Dec. 2009.

[28] J. Renaudier, O. Bertran-Pardo, M. Salsi, F. Vacondio, H. Mardoyan, P. Tran, G. Charlet, and S. Bigo, "Tolerance to nonlinearity of 40 Gb/s BPSK-based coherent solution over legacy systems based on non-zero dispersion-shifted fibers," presented at the Opt. Fiber. Commun. Conf., Los Angeles, CA, 2011, Paper OThX3.

[29] J.-C. Antona, M. Lefrançois, S. Bigo, and G. Le Meur, "Investigation of advanced dispersion management techniques for ultra-long haul transmissions," presented at the Eur. Conf. Opt. Commun., Glasgow, U.K., 2005, Paper Mo.3.2.6.

[30] M. Bertolini, P. Serena, G. Bellotti, and A. Bononi, "On the XPM-induced distortion in DQPSK-OOK and coherent QPSK-OOK hybrid systems," presented at the Opt. Fiber Commun. Conf., San Diego, CA, 2009, Paper OTuD4.

[31] J. Renaudier, O. Bertran-Pardo, H. Mardoyan, P. Tran, M. Salsi, G. Charlet, S. Bigo, M. Lefrançois, B. Lavigne, J.-L. Auge, L. Piriou, and O. Courtois, "Performance comparison of 40 G and 100 G coherent PDM-QPSK for upgrading dispersion managed legacy systems," presented at the Nat. Fiber Opt. Eng. Conf., San Diego, CA, 2009, Paper NWD5.

[32] G. Bellotti, M. Varani, C. Francia, and A. Bononi, "Intensity distortion induced by cross-phase modulation and chromatic dispersion in optical- fiber transmissions with dispersion compensation," *IEEE Photon. Technol. Lett.*, vol. 10, no. 12, pp. 733–736, Dec. 1998.

[33] C. Fürst, J.-P. Elbers, C. Scheerer, and C. Glingener, "Limitations of dispersion-managed DWDM systems due to cross-phase modulation," in *Proc. 13th Annu. Meet. Laser Electro-Opt. Soc.*, Rio Grande, Puerto Rico, 2000, pp. 23–24.

[34] M. R. Phillips and S. L. Woodward, "Cross-polarization modulation: Theory and measurement of a two-channel WDM system," *IEEE Photon. Technol. Lett.*, vol. 17, no. 10, pp. 2086–2088, Oct. 2005.

[35] B. C. Collings and L. Boivin, "Nonlinear polarization evolution induced by cross-phase modulation and its impact on optical transmission systems," *IEEE Photon. Technol. Lett.*, vol. 12, no. 11, pp. 1582–1584, Nov. 2000.

[36] D. Van den Borne, N. E. Hecker-Denschlag, G.-D. Khoe, and H. De Waardt, "Cross phase modulation induced depolarization penalties in 2×10 Gb/s polarization-multiplexed transmission," presented at the presented at the Eur. Conf. Opt. Commun., Stockholm, Sweden, 2004, Paper Mo.4.5.5.

[37] G. Charlet, M. Salsi, H. Mardoyan, P. Tran, J. Renaudier, S. Bigo, M. Astruc, P. Sillard, L. Provost, and F. Cérou, "Transmission of 81 channels at 40 Gbit/s over a transpacific-distance erbium-only link, using PDM-BPSK modulation, coherent detection, and a new large effective area fibre," presented at the Eur. Conf. Opt. Commun., Brussels, Belgium, Paper Th3E3.

[38] M. Salsi, G. Charlet, O. Bertran-Pardo, J. Renaudier, H. Mardoyan, P. Tran, and S. Bigo, "Experimental comparison between binary and quadrature phase shift keying at 40 Gbit/s in a transmission system using coherent detection," presented at the Eur. Conf. Opt. Commun., Torino, Italy, 2010, Paper Mo.2.C.5.

[39] V. Sleiffer, M. Alfiad, D. van den Borne, S. Jansen, M. Kuschnerov, S. Adhikari, and H. de Waardt, "A comparison of 43-Gb/s POLMUX-RZ-DPSK and POLMUX-RZ-DQPSK modulation for long-haul transmission systems," presented at the Eur. Conf. Opt. Commun., Torino, Italy, Paper Mo.2.C.4.

[40] M. Yan, H. Zhang, W. Yan, P. R. T. Hoshida, and J. C. Rasmussen, "Adaptive blind equalization for coherent optical BPSK system," presented at the Eur. Conf. Opt. Commun., Torino, Italy, Paper Th.9.A.4.

[41] D. N. Godard, "Self-recovering equalization and carrier tracking in two-dimensional data communication systems," *IEEE Trans. Commun.*, vol. COM-28, no. 11, pp. 1867–1875, Nov. 1980.

[42] A. J. Viterbi and A. M. Viterbi, "Nonlinear estimation of PSK-modulated carrier phase with application to burst digital transmission," *IEEE Trans. Inf. Theory*, vol. IT-29, no. 4, pp. 543–551, Jul. 1983.

[43] A. Leven, N. Kaneda, U.-V. Koc, and Y.-K. Chen, "Frequency estimation in intradyne reception," *IEEE Photon. Technol. Lett.*, vol. 19, no. 6, pp. 366–368, Mar. 2007.

Author biographies not included at author request due to space constraints.